DMD Fast Forward. Published on April 30, 2007 as doi:10.1124/dmd.107.015230

Atorvastatin Glucuronidation is Minimally and Non-Selectively Inhibited by the Fibrates Gemfibrozil, Fenofibrate and Fenofibric Acid

Theunis C. Goosen, Jonathan N. Bauman, John A. Davis[1], Chongwoo Yu[2], Susan I. Hurst, J. Andrew Williams, and Cho-Ming Loi

Department of Pharmacokinetics, Dynamics and Metabolism, Pfizer Global Research and Development, Ann Arbor, Michigan

Running Title. Modulation of Atorvastatin Glucuronidation by Fibrates

Address correspondence to: Theunis C. Goosen, Department of Pharmacokinetics, Dynamics and Metabolism, Pfizer Global Research and Development, 2800 Plymouth Rd., Ann Arbor, MI 48105. Phone: (734) 622-5752, Fax: (734) 622-4349, Email: theunis.goosen@pfizer.com

Number of text pages: 36

Number of tables: 3

Number of figures: 8

Number of references: 40

Number of words in Abstract: 250

Number of words in Introduction: 724

Number of words in Discussion: 1421

Abbreviations: amu, atomic mass unit(s); β-RAM, radioactivity monitor; CID, collision induced dissociation; ESI, electrospray ionization; G1, atorvastatin ether glucuronide; G2, atorvastatin acyl glucuronide; G3, atorvastatin lactone ether glucuronide; HFC, 7-hydroxy-4-trifluoromethylcoumarin; HLM, human liver microsomes; HMG-CoA, 3-hydroxy-3-methylglutaryl-coenzyme A; IS; internal standard; LC, liquid chromatography; MS, mass spectrometry; MS/MS, tandem mass spectrometry; UDPGA, uridine 5'-diphosphoglucuronic acid; UGT, UDP-glucuronosyltransferase; UV, ultraviolet.

ABSTRACT

Gemfibrozil co-administration generally results in plasma statin AUC increases, ranging from moderate (2- to 3-fold) with simvastatin, lovastatin and pravastatin to most significant with cerivastatin (5.6-fold). Inhibition of statin glucuronidation has been postulated as a potential mechanism of interaction (Prueksaritanont et al. (2002) Drug Metab Dispos 30:1280-7). This study was conducted to determine the in vitro inhibitory potential of fibrates towards atorvastatin glucuronidation. [^{3}H]atorvastatin, atorvastatin, and atorvastatin lactone were incubated with human liver microsomes (HLM) or human recombinant UDP-glucuronosyltransferases (UGTs) and characterized using LC/MS/MS and LC/UV/β-RAM/MS. [^{3}H]Atorvastatin yields a minor ether glucuronide (G1) and a major acyl glucuronide (G2) with subsequent pH-dependent lactonization of G2 to yield atorvastatin lactone. Atorvastatin lactonization best fit substrate inhibition kinetics (K_m = 12 μM, V_{max} = 74 pmol/min/mg, K_i = 75 μM). Atorvastatin lactone yields a single ether glucuronide (G3). G3 formation best fit Michaelis-Menten kinetics (K_m = 2.6 μM, V_{max} = 10.6 pmol/min/mg). Six UGT enzymes contribute to atorvastatin glucuronidation with G2 and G3 formation catalyzed by UGTs 1A1, 1A3, 1A4, 1A8, and 2B7 while G1 formation was catalyzed by UGTs 1A3, 1A4, and 1A9. Gemfibrozil, fenofibrate, and fenofibric acid inhibited atorvastatin lactonization with IC_{50}-values of 346 μM, 320 μM, and 291 μM, respectively. Based on unbound fibrate concentrations at the inlet to the liver, these data predict a small increase in atorvastatin AUC (~ 1.2-fold) following gemfibrozil co-administration and no interaction with fenofibrate. This result is consistent with recent clinical reports indicating minimal atorvastatin AUC increases (~ 1.2- to 1.4-fold) with gemfibrozil.

Atorvastatin calcium is the most widely used 3-hydroxy-3-methylglutaryl-coenzyme A (HMG-CoA) reductase inhibitor (statin) in the United States. Statins are considered first-line therapeutic agents for the prevention of coronary heart disease and atherosclerotic disorders related to hypercholesterolemia (Grundy et al., 2004). These drugs are generally well tolerated with established benefit as cholesterol lowering agents (Newman et al., 2003; Bays, 2006; Guyton, 2006). Drug-drug interactions have been described during combination therapy between fibric acid derivatives (fibrates), particularly gemfibrozil, and several statins (Bottorff, 2006). Combination therapy with statins and fibrates is a promising approach in the treatment of patients with mixed hyperlipidemia since statins primarily reduce low-density lipoprotein (LDL) while fibrates reduce triglycerides and increase high density lipoprotein (HDL) levels with established reduction in cardiovascular morbidity (Rubins et al., 1999; Grundy et al., 2004; Vasudevan and Jones, 2006). Nevertheless, the relative potential for fibrates to interact with statins, particularly atorvastatin, necessitates further understanding.

Clinically, it has been shown that compared to monotherapy, gemfibrozil resulted in the most significant increases in hydroxy acid statin AUC (>5-fold) when co-administered with cerivastatin (Backman et al., 2002), while AUC changes were moderate (2- to 5-fold) following co-administration with simvastatin (Backman et al., 2000), lovastatin (Kyrklund et al., 2001), and pravastatin (Kyrklund et al., 2003). Smaller changes in statin AUC (1.25- to 2-fold) were observed for rosuvastatin (Schneck et al., 2004) and pitavastatin (Mathew et al., 2004). A similar pharmacokinetic interaction has not been observed with fluvastatin (Spence et al., 1995) and, except for a metabolite of pravastatin (Pan et al., 2000), is generally not observed during statin co-administration with other fibrates (fenofibrate or bezafibrate) (Kyrklund et al., 2001; Martin et al., 2003; Bergman et al., 2004). The relative potential for gemfibrozil to have a

pharmacokinetic drug-drug interaction with atorvastatin was however, until recently, not known (Backman et al., 2005; Whitfield et al., 2005).

The mechanistic basis for the gemfibrozil-statin drug interaction is not clear, although it is generally accepted to comprise a pharmacodynamic and possibly also a pharmacokinetic component, since gemfibrozil related adverse events mirror those observed for statins and combination therapy may result in increased statin exposure with apparent dose-related increases in adverse events (Law and Rudnicka, 2006). Since many statins that exhibit a pharmacokinetic interaction with gemfibrozil are at least partially cleared by CYP3A4 and gemfibrozil is not a CYP3A4 inhibitor, recent in vitro experiments published in the literature speculated that inhibition of statin glucuronidation by gemfibrozil but not fenofibrate may be involved (Prueksaritanont et al., 2002b; Prueksaritanont et al., 2002c). Furthermore, a novel mechanism for statin lactonization mediated through glucuronidation was described (Prueksaritanont et al., 2002a), although in vitro differential interaction of fibrates on atorvastatin glucuronidation is not clearly defined.

Pharmacokinetic interactions between statins and gemfibrozil are clearly complex since multiple clearance mechanisms for statins exist including oxidative metabolism by cytochrome P450s (CYPs), phase II metabolism by UDP-glucuronosyltransferases (UGTs), intestinal and hepatic uptake clearance by multiple transporters, and interconversion kinetics between statin hydroxy acid and their corresponding lactone forms (Shitara and Sugiyama, 2006). Atorvastatin is subject to first-pass metabolism, mainly mediated by CYP3A4, resulting in the formation of two hydroxylated active metabolites (Jacobsen et al., 2000; Lennernas, 2003). Atorvastatin (active hydroxy acid form) is also biotransformed to atorvastatin lactone (Fig. 1), which could occur non-enzymatically at low intestinal pH (Kearney et al., 1993) or via a coenzyme-A (Li et

al., 2006) or acyl glucuronide intermediate pathway (Prueksaritanont et al., 2002a). Additionally, atorvastatin is also a substrate for several transport proteins including the efflux transporter P-glycoprotein (Wu et al., 2000), hepatic uptake organic anion transporting polypeptide 1B1 (OATP1B1; also known as OATP-C or OATP2) (Chen et al., 2005), and a proton-monocarboxylic acid cotransporter (MCT) (Wu et al., 2000). The relative importance of these clearance mechanisms for atorvastatin is not fully understood. Nevertheless, a significant role for OATP1B1 and CYP3A4 in atorvastatin clearance is implied based on clinical drug-drug interactions with inhibitors such as single-dose rifampin and itraconazole, respectively (Backman et al., 2005; Bottorff, 2006; Lau et al., 2007).

In order to increase the current understanding of the potential differential inhibitory effect of fibrates on atorvastatin glucuronidation, the purpose of this study was to characterize atorvastatin glucuronidation in human liver microsomes, evaluate human recombinant UGTs that mediate atorvastatin glucuronidation, and determine the in vitro potential of gemfibrozil, fenofibrate and its active metabolite, fenofibric acid, to modulate or inhibit atorvastatin glucuronidation.

Materials and Methods

Materials. Atorvastatin calcium and atorvastatin lactone were synthesized by the Department of Chemistry, Pfizer Inc (Ann Arbor, MI). [^{3}H]Atorvastatin (7.3 Ci/mmol, 99.4% pure) was synthesized by Pharmaceutical Sciences, Pfizer Inc (Kalamazoo, MI). Fenofibric acid was supplied by Tyger Scientific, Inc (Ewing, NJ) and eugenol was supplied by Alfa Aesar (Ward Hill, MA). Pooled human liver microsomes (mixed gender, N = 60) and recombinant baculovirus-derived microsomes expressing human UGT (vector control, UGTs 1A1, 1A3, 1A4, 1A6, 1A7, 1A8, 1A9, 1A10, 2B4, 2B7, 2B15, and 2B17) were obtained from BD Gentest (Woburn, MA). All other chemicals were commercially available and of analytical grade from Sigma-Aldrich (St. Louis, MO).

UGT-Catalyzed Metabolism of [^{3}H]Atorvastatin in Human Liver Microsomes. Pooled human liver microsomes (1.0 mg/mL), 50 mM Tris-HCl buffer (pH 7.0 at 37°C), 5 mM $MgCl_2$, and alamethicin (50 μg/mg protein) were pre-incubated (on ice for 15 min) before addition of [^{3}H]atorvastatin (10 μM, 2.1 μCi) in a final incubation volume of 200 μL and pre-incubated at 37°C for 3 min. Reactions were initiated with UDPGA (5 mM). After incubation for 60 min at 37°C, reactions were quenched on ice for 30 min with 100 μL of 5% glacial acetic acid in acetonitrile (final pH = 3.5) containing lovastatin as internal standard. Quenched incubates were centrifuged at 12000 rpm for 10 minutes before analysis of supernatants by LC-UV/β-RAM/MS as described below. Stability of quenched incubates were evaluated by sequential injections from the autosampler held at ambient room temperature over a period of approximately 21 hr. Product amounts were quantified based on radiolabeled equivalents and expressed as a percent of initial concentration. Glucuronides were identified by LC-MS/MS

DMD Fast Forward. Published on April 30, 2007 as DOI: 10.1124/dmd.107.015230
This article has not been copyedited and formatted. The final version may differ from this version.

from incubations containing unlabeled atorvastatin (10 μM) or atorvastatin lactone (10 μM) as described below.

Enzyme Kinetics of Atorvastatin and Atorvastatin Lactone Glucuronidation. For determination of enzyme kinetic parameters, incubations containing 0.25 mg/mL HLM were incubated with increasing concentrations (0.1 – 300 μM in 0.5% DMSO final) of atorvastatin or atorvastatin lactone for 60 min as described above. Preliminary experiments evaluating linearity of product formation with respect to human liver microsomal protein (0.1-1.5 mg/mL) and time (15-90 min) at a substrate concentration (1.8 μM) below the apparent K_m indicated that product formation was linear with protein concentration up to 0.75 mg/mL for up to 90 min. Supernatants were analyzed by HPLC and glucuronides were quantified by UV detection.

Substrate concentration [S] and velocity (V) data were fitted to the appropriate enzyme kinetic model by nonlinear least-squares regression analysis (Sigmaplot; SPSS, Chicago, IL) in order to derive the apparent enzyme kinetic parameters V_{max} (maximal velocity) and K_m or S_{50} (substrate concentration at half-maximal velocity). The Michaelis-Menten model (eq. 1), the uncompetitive substrate inhibition model (eq. 2), the two-enzyme model (eq. 3), and the substrate activation model (eq. 4), which incorporates the Hill coefficient (n), were used:

$$V = V_{max} \times S / (K_m + S) \quad (1)$$

$$V = V_{max} \times S / (K_m + S \times (1 + S/K_i)) \quad (2)$$

$$V = V_{max1} \times S / (K_{m1} + S) + V_{max2} \times S / (K_{m2} + S) \quad (3)$$

$$V = V_{max} \times S^n / (S_{50}{}^n + S^n) \quad (4)$$

where V_{max} is the maximal velocity, K_m or S_{50} is the substrate concentration at half-maximal velocity, n is an exponent indicative of the degree of curve sigmoidicity, and K_i is an inhibition constant. The best fit was based on a number of criteria, including visual inspection of the data

plots (Michaelis-Menten and Eadie-Hofstee), distribution of the residuals, size of the sum of the squared residuals, and the standard error of the estimates. Selection of models other than Michaelis-Menten was based on the F-test ($P < 0.05$) and the Akaike Information Criterion (AIC).

Role of UGT Enzymes in Atorvastatin Glucuronidation. Atorvastatin or atorvastatin lactone (1 μM, 10 μM or 100 μM in 0.5% DMSO) were incubated with recombinantly expressed human UGTs (0.5 mg/mL) as described for HLM. Incubations (200 μL) were quenched (60 min) with 50 μL of 5% glacial acetic acid in acetonitrile containing 125 ng/mL lovastatin on ice for 30 min. Supernatants were carefully removed for LC-MS/MS analysis as described below. Results were expressed as peak area of product/internal standard ratio obtained from LC-MS/MS analyses. Positive control incubations with recombinant enzymes were performed as above using β-estradiol (UGT1A1 and UGT1A3), trifluoperizine (UGT1A4), HFC (UGTs 1A6, 1A7, 1A8, 1A9, 1A10, 2B4, 2B7 and 2B15) and eugenol (UGT2B17) as substrates to confirm active enzyme in incubations.

Inhibition of Atorvastatin and Atorvastatin Lactone Glucuronidation by Fibrates. To determine inhibition of atorvastatin or atorvastatin lactone glucuronidation by gemfibrozil, fenofibrate or fenofibric acid, HLM (0.5 mg/mL) were incubated with atorvastatin (12 μM) or atorvastatin lactone (2.5 μM) at or below its respective K_m concentration together with increasing concentrations (0.03 – 1000 μM in 0.5% DMSO) of gemfibrozil, fenofibrate or fenofibric acid. Control incubations contained DMSO (0.5% final), without inhibitor. Quenched aliquots containing 125 ng/mL lovastatin (IS) were analyzed by LC-MS/MS and results were compared to aliquots supplemented with internal standard (40 ng lovastatin) analyzed by LC-UV. IC_{50}

values calculated using both LC-MS/MS and LC-UV were comparable and final data are presented from LC-MS/MS analyses, due to superior analyte selectivity and sensitivity.

IC_{50} estimates for inhibition of glucuronidation were determined by nonlinear curve fitting with GraphPad Prizm (GraphPad Software, San Diego, CA), and were defined as the concentration of inhibitor required to inhibit control glucuronidation reactions by 50%.

Analytical Procedures for Atorvastatin and Metabolites. Atorvastatin, atorvastatin lactone and their corresponding glucuronide(s) were characterized by liquid chromatography-tandem mass spectrometry (LC-MS/MS) using an Applied Biosystems/MDS Sciex (Concord, ON, Canada) model API 4000 triple quadrupole mass spectrometer. For LC-MS/MS profiling and identification of glucuronide(s) formed, aliquots (25 µl) of the supernatants from in vitro HLM incubations with either atorvastatin or atorvastatin lactone as substrate were injected onto a HPLC column (Waters, Xterra, MS C_{18}, 5µ, 2.1 x 100 mm; Waters, Milford, MA). The HPLC system consisted of an Agilent 1100 HPLC pump and CTC Analytics PAL autosampler maintained at 5°C. The mobile phase was 10 mM ammonium acetate pH 4.5 (A) and acetonitrile (B) at a flow rate of 0.25 mL/min. Initial solvent conditions were 30% B held for 1 min, increased linearly to 75% B over 16 min and run isocratically for 2 min, followed by a return to initial conditions in 1 min and re-equilibration for 5 min. The mass spectrometer was operated using an ESI interface in the positive ion mode (5000 eV; 300 °C).

Quantification of atorvastatin, atorvastatin lactone, and relative quantities of their corresponding glucuronides were determined following injection of supernatant (10 µL) on the same LC-MS/MS system described above except the flow rate was 0.3 mL/min. Initial solvent conditions were 35% B followed by a linear increase to 50% B in 2 min, followed by an increase to 75% B in 0.01 min where these conditions were held for 1.99 min, followed by another

increase to 95% B in 0.01 min where these conditions were held for 1.99 min, with a return to initial conditions in 0.01 min and a re-equilibration time of 4.99 min. The collision energies and multiple reaction monitoring (MRM) transitions were as follows: atorvastatin (31 eV, 559.2 → 440.3), atorvastatin lactone (28 eV, 541.3 → 448.3), atorvastatin glucuronides (G1 and G2; 31 eV, 735.2 → 559.2), atorvastatin lactone glucuronide (G3; 28 eV, 717.3 → 624.3) and lovastatin (IS, 23 eV, 422.2 → 199.2). Atorvastatin and atorvastatin lactone were quantified based on standard curves using authentic standards. Glucuronide amounts were expressed as an area ratio of analyte/internal standard in the absence of authentic standards, except for determination of enzyme kinetic parameters where LC-UV analyses were used as described below. Standards were prepared in HLM or UGT cDNA matrix, containing all reagents included in incubation except UDPGA, with standard concentrations starting at the lower limit of quantification (LOQ) and ranging 0.25 – 10 000 ng/mL for LC-MS/MS analyses and 5 – 15 000 ng/mL for LC-UV analyses, and with the range depending on the experiment of interest. Standards were quenched similar to samples as reported above.

LC-UV/β-RAM/MS analyses were performed in order to evaluate relative glucuronide quantities, metabolite stabilities, and enzyme kinetic parameters. Aliquots of the supernatant (100 µL) from [^{3}H]atorvastatin or unlabeled substrate incubations were monitored by UV absorption at 245 nm, an on-line β-RAM radioactivity detector (IN/US Systems, Tampa, FL), and/or a LCQ Advantage ion trap mass spectrometer (ThermoFinnigan, San Jose, CA). Aliquots were injected onto a HPLC column (Luna $C_{18(2)}$, 100A, 5-µm, 4.6 x 150 mm; Phenomenex, Torrance, CA) and separated with a mobile phase of 10 mM ammonium acetate pH 4.5 (A) and acetonitrile (B) at a flow rate of 1 mL/min. Initial conditions were held at 30% B for 0.5 min followed by a linear increase to 75% B in 15.5 min, returning to initial conditions at 16.5 min.

Mass spectral analyses were performed using ESI in the positive ion mode with ionization voltage at 1 kV and the heated capillary temperature held at 300 °C. Atorvastatin and atorvastatin lactone were quantified based on a standard curve using authentic standards. In the absence of authentic standards for glucuronide metabolites, the UV absorption at 245 nm relative to the radiolabel was determined and compared to parent substrate. Since it was established that the UV:[^{3}H] relationship was essentially directly proportional (1:1), glucuronide products were subsequently quantified by UV absorbance for enzyme kinetic experiments, based on standard curves generated with the parent aglycone.

Prediction of Drug-Drug Interaction Potential. The effects of fibrate co-administration on atorvastatin AUC were predicted based on observed in vitro inhibitory potencies and fibrate plasma exposures, using published methodology for predicting drug-drug interactions based on in vitro enzyme inhibition for cytochrome P450 enzymes (Kanamitsu et al., 2000; Brown et al., 2005). For predictions based on total (bound and unbound) or unbound fibrate maximal plasma concentration (C_{max}) at steady state, a modified version of the equation developed by Rowland and Matin (Rowland and Matin, 1973) was used:

$$\frac{AUC_i}{AUC} = \frac{1}{\frac{f_m \cdot f_{m,UGT}}{1+[I]/K_i} + (1 - f_m \cdot f_{m,UGT})} \quad (5)$$

where AUC_i/AUC represents the AUC ratio in the presence and absence of an inhibitor (predicted change in AUC), $[I]$ is inhibitor concentration, K_i is a constant describing affinity of inhibitor for the enzyme (assuming competitive inhibition $K_i = IC_{50}/2$), f_m is the fraction of drug cleared by metabolism (as opposed to renal or biliary excretion of unchanged drug), and $f_{m,UGT}$ is the fraction of drug metabolized by UGT enzymes. Although $f_{m,UGT}$ for atorvastatin in humans is

not known, a value of 0.8 was assumed to represent the most conservative estimate for predicting an interaction of greatest possible magnitude.

In order to evaluate the effect of the unbound hepatic drug concentration at the inlet to the liver ($[I]_{in}$), unbound inhibitor concentrations were calculated using the following equation:

$$[I]_{in} = f_u([I]_{max} + k_a \cdot F_a \cdot \frac{D}{Q_H}) \quad (6)$$

Where $[I]_{max}$ is the maximum systemic plasma concentration (C_{max}) of inhibitor drug, k_a is the absorption rate constant, F_a the fraction of the dose absorbed from the gastrointestinal tract, D the inhibitor dose and Q_H the hepatic blood flow (1450 mL/min). For unbound fractions, f_u = 0.02 and f_u = 0.01 was used for gemfibrozil and fenofibric acid, respectively (Miller and Spence, 1998). Gemfibrozil and fenofibric acid plasma concentratrions and terminal elimination half-lives were from reported literature values (Whitfield et al., 2005). For these predictions F_a was assumed as 1 and k_a was estimated from inhibitor pharmacokinetic data using the following equation:

$$t_{max} = \frac{\ln(k_a / k_e)}{k_a - k_e} \quad (7)$$

where t_{max} is time to reach C_{max}, and k_e is the elimination rate constant obtained from the elimination half-life ($t_{½} = 0.693/k_e$). Employing gemfibrozil and fenofibric acid terminal $t_{½}$ of 2.4 h and 22.7 h, estimates for gemfibrozil and fenofibrate k_a were 1.2 min^{-1} and 1.1 min^{-1}, respectively.

Results

UGT-Mediated Atorvastatin Metabolism. Atorvastatin glucuronidation resulted in the formation of atorvastatin lactone as major metabolite and three glucuronide conjugates (Fig. 1.) [^{3}H]atorvastatin was glucuronidated and following acetic acid quench (pH 3.5), yielded atorvastatin lactone as the major metabolite accounting for 64% of total product, a major atorvastatin acyl glucuronide conjugate (G2) and a minor ether glucuronide conjugate (G1) respresenting 32% and 4% of total product, respectively (Fig. 2). Atorvastatin lactone, in turn, is also glucuronidated and yields a single atorvastatin lactone ether glucuronide conjugate (G3), following incubation of atorvastatin lactone as substrate, as shown in Fig. 2. The rate of G3 formation was low following incubation with [^{3}H]atorvastatin and although chromatographically separated, was not detected in the radioactive trace, but could be detected by LC-MS/MS due to superior sensitivity. Following incubation with atorvastatin lactone, atorvastatin and its glucuronides (G1 and G2) were also detected by LC-UV and LC-MS/MS analyses, respectively. The non-enzymatic conversion of atorvastatin lactone to atorvastatin was confirmed under the physiological pH incubation conditions.

The major atorvastatin acyl glucuronide (G2) was unstable under physiological pH and spontaneously lactonized to yield atorvastatin lactone. Atorvastatin lactonization was incomplete under our incubation conditions (pH = 7.0) and was quenched by addition of acetic acid (pH = 3.5) preventing further conversion of G2 to atorvastatin lactone prior to analysis. Under these conditions, formation of G2 was approximately 32%. For stability analyses, the glucuronidation products of atorvastatin, quenched with acetic acid to stop conversion to atorvastatin lactone, were stable for at least 21 hours at ambient room temperature. The mean change (percent, % CV) in product amounts expressed as a percentage of initial concentration

(mean of first two injections) directly following acetic acid quench were: G1 (11.6, 9.2); G2 (-1.7, 4.9); atorvastatin (-0.1, 0.7); atorvastatin lactone (8.0, 5.2). The product amounts did not change by more than 11.6% of initial amounts and the coefficients of variation were less that 9.2%. The chemical conversion of atorvastatin to atorvastatin lactone incubated without UDPGA was minimal, typically less than 1%.

Glucuronide Structure Elucidation. The structures of glucuronide conjugates as characterized by LC-MS/MS are depicted in Fig. 3. The collision induced dissociation (CID) product ion spectrum for atorvastatin shows a protonated molecular ion of m/z 559 (Fig. 3, panel A). The major ions of interest in the spectrum include m/z 466 representing the loss of the aniline moiety and m/z 440 representing the loss of the phenyl-amino-carbonyl moiety.

The CID product ion spectrum of G2 shows a protonated molecular ion of m/z 735 (Fig. 3, panel C). The two atorvastatin glucuronides (G1 and G2) had nearly identical CID product ion spectra and since G2 was produced in greater quantities than G1, a representative CID spectrum for this metabolite is shown. As shown in Fig. 3 panel C, the major fragment formed is the characteristic loss of 176 amu seen with glucuronides forming the aglycone, atorvastatin at m/z 559. Major fragments of interest include m/z 642 representing the loss of the aniline moiety from the parent glucuronide molecule, as well as m/z 466, which is 176 amu less than m/z 642, which represents the loss of the glucuronide moiety as well as the loss of the aniline moiety from G2. The structure of G2 would correspond to the 1-O-acyl-β-D-glucuronide of atorvastatin previously described and characterized by nuclear magnetic resonance (Prueksaritanont et al., 2002a). G1 is proposed to be the aliphatic ether glucuronide of atorvastatin.

The CID product ion spectrum for atorvastatin lactone is depicted in Fig. 3 panel B and shows a protonated molecular ion of m/z 541. The major ions of interest in the spectrum include

m/z 448 representing the loss of the aniline moiety and m/z 422 representing the loss of the phenyl-amino-carbonyl moiety. The CID product ion spectrum of G3 (Fig. 3, panel D) shows a protonated molecular ion of m/z 717. The proposed ether glucuronide conjugate exhibits the characteristic loss of 176 amu seen with glucuronides forming the aglycone, atorvastatin lactone at m/z 541. The fragments of interest include m/z 624, representing the loss of the aniline moiety and m/z 448, which is 176 amu less than m/z 624 and represents the loss of glucuronide as well a loss of aniline from G3.

Enzyme Kinetics of Atorvastatin and Atorvastatin Lactone Glucuronidation. The apparent enzyme kinetic parameters for glucuronidation of atorvastatin and atorvastatin lactone are summarized in Table 1 and shown graphically in Fig. 4- Fig 6. Separate kinetic parameters were determined with either atorvastatin or atorvastatin lactone as substrates to best characterize kinetically the proposed glucuronidation pathways of atorvastatin resulting in the formation of three glucuronides and atorvastatin lactone (Fig. 1).

The lactonization of atorvastatin (formation of G2 followed by spontaneous degradation to atorvastatin lactone) implies a single-step enzymatic reaction. Therefore, for atorvastatin lactonization kinetic parameters (particularly V_{max}), product amounts of G2 and atorvastatin lactone were summed. Atorvastatin lactonization best fit a substrate inhibition model as evidenced by the Eadie-Hofstee plot (Fig. 4, insert). Higher atorvastatin substrate concentrations (> 100 μM) were not fitted to the kinetic model (Fig. 4) since atorvastatin contains low levels of atorvastatin lactone (< 1%). This leads to ambiguity in the amount of atorvastatin lactone formed enzymatically when greater than 100 μM atorvastatin was incubated with HLM. This observation was further complicated by apparent substrate inhibition kinetics for atorvastatin lactonization, which was clearly apparent when [S] against V data is plotted for G2 formation up

DMD Fast Forward. Published on April 30, 2007 as DOI: 10.1124/dmd.107.015230
This article has not been copyedited and formatted. The final version may differ from this version.

to 300 μM atorvastatin (Fig. 5). No further attempts were made to characterize the potential role of product inhibition (eg atorvastatin lactone) to these kinetic observations. Although not appropriate to define enzyme kinetic parameters (particularly V_{max}) for atorvastatin lactonization, the K_m obtained for G2 formation was comparable to the K_m for the two-step lactonization process (Table 1). The levels of G1 formation at lower substrate concentration were not adequately quantifiable by LC-UV analyses to estimate kinetic parameters for its formation. In incubations with atorvastatin as substrate, levels of G3 were generally not detected with LC-UV or radiolabel detection methods but could be detected by LC-MS/MS.

The simple Michaelis-Menten model adequately described the glucuronidation of atorvastatin lactone (Fig. 6). As shown in Table 1, the K_m for G3 formation from atorvastatin lactone (2.6 μM) was 4.6-fold lower than that obtained for atorvastatin lactonization (12 μM). However, the intrinsic clearance (CL_{int}) values for atorvastatin lactonization and atorvastatin lactone glucuronidation in HLM were comparable, 6.2 and 4.2 μL/min/mg, respectively. Since atorvastatin lactone hydrolyzes under physiological pH to form atorvastatin, atorvastatin and its two glucuronides (G1 and G2) were also detected in incubations with atorvastatin lactone but were not quantified.

In the absence of authentic glucuronide standards, glucuronide amounts were quantified for enzyme kinetic experiments based on the UV absorbance since the UV absorbance/radiolabel response relationship for the atorvastatin glucuronides calculated from LC-UV/β-RAM experiments were essentially 1:1 (mean ratio ± standard deviation calculated from 16 injections was 1.03 ± 0.16 and 0.95 ± 0.08 for G1 and G2, respectively).

Atorvastatin and Atorvastatin Lactone Glucuronidation Incubated with Recombinant UGTs. The ability of recombinant human UGTs to glucuronidate atorvastatin

and atorvastatin lactone is summarized in Fig. 7. The highest rates of G1 formation were catalyzed by UGT1A3 and UGT1A4. Lower activity for G1 formation was also detected at higher atorvastatin substrate concentrations (≥ 10 μM) with UGT1A9.

The highest rates of G2 formation were catalyzed by UGT1A1 and UGT1A3. Lower glucuronidation activities for G2-formation were also detected with UGTs 1A4, 1A8 and 2B7. UGT1A4 and UGT1A8 catalyzed glucuronidation was only detected at higher atorvastatin substrate concentrations (≥ 10 μM).

G3 formation was mainly catalyzed by UGT1A3 and UGT1A4. Lower activities were also observed with UGTs 1A1, 1A8 and 2B7. Analysis of positive controls revealed that all recombinant enzymes were active during the incubations.

Inhibition of Atorvastatin and Atorvastatin Lactone Glucuronidation by Gemfibrozil, Fenofibrate and Fenofibric Acid. The ability of gemfibrozil, fenofibrate or its active metabolite, fenofibric acid, to inhibit atorvastatin or atorvastatin lactone glucuronidation in HLM is summarized in Table 2 and Fig. 8. As shown in and Fig. 8, panel A, the formation of G1 increased approximately 1.6-fold in the presence of 600 μM gemfibrozil, compared to controls without gemfibrozil. The mean increase was maximal in the presence of 600 μM gemfibrozil with no difference from control at 1000 μM. The lactonization of atorvastatin (Fig. 8, panel B) was inhibited by gemfibrozil with an IC_{50} value of 346 μM. G3 formation from incubations with atorvastatin lactone as substrate was not significantly inhibited by gemfibrozil.

Fenofibrate and its active metabolite, fenofibric acid, similarly increased G1 glucuronidation of atorvastatin approximately 6.7-fold and 9.5-fold, respectively, at 1000 μM, compared to control values (Table 2 and Fig. 8, panel D). The lactonization of atorvastatin was similarly inhibited by fenofibrate and fenofibric acid with IC_{50} values of 320 μM and 291 μM,

respectively. All inhibitors appeared soluble at higher concentration, which is supported by increasing inhibitor concentrations resulting in decreased enzyme activity through 1000 μM (Fig. 8, panels B, E).

In contrast to gemfibrozil, the in vitro glucuronidation of atorvastatin lactone (G3) was inhibited by fenofibrate and fenofibric acid (Fig. 8, panel F). The mean inhibition of G3 formation was 45 ± 0.7% and 50 ± 2.4% at fenofibrate and fenofibric acid concentrations of 1000 μM, respectively. The fitted IC_{50}-values for inhibition of atorvastatin lactone glucuronidation were therefore slightly higher than 1000 μM.

Prediction of Drug-Drug Interaction Potential. The predicted in vivo effects of fibrates on human atorvastatin AUC is summarized in Table 3. For both gemfibrozil and fenofibrate, the predicted increase in atorvastatin AUC was considered to be minimal.

Discussion

The findings presented here describe the relatively weak and non-selective inhibition of atorvastatin glucuronidation by gemfibrozil and fenofibrate, the major fibrates prescribed in the United States, as well as characterization of the in vitro glucuronidation of atorvastatin and its lactone metabolite. Based on these findings, the predicted change in human atorvastatin AUC during gemfibrozil or fenofibrate co-administration is minimal.

Following administration of atorvastatin calcium, atorvastatin lactone is commonly detected in human plasma with comparable AUC exposure to atorvastatin (Kantola et al., 1998). The relative contribution of possible pathways responsible for atorvastatin lactone formation is not clear, but may involve acid-catalyzed formation at low intestinal pH prior to absorption (Kearney et al., 1993), or enzymatic formation mediated through acyl glucuronide formation (Prueksaritanont et al., 2002a), or via a coenzyme-A dependent pathway (Li et al., 2006). Since the base-catalyzed formation of atorvastatin from the lactone would be essentially irreversible at higher pH, enzymatic formation of atorvastatin lactone would likely be dominant under physiological pH. The in vitro UGT-catalyzed metabolism of atorvastatin in HLM presented here indicates that atorvastatin lactone is a major metabolite and that its formation is mediated through acyl glucuronide (G2) formation. Additionally, the formation of a single atorvastatin lactone glucuronide (G3) and a minor atorvastatin ether glucuronide (G1) was characterized. Following administration of [^{14}C]atorvastatin in patients with a T-tube, biliary excretion was the major elimination route with unchanged atorvastatin, *ortho*-hydroxy atorvastatin, *para*-hydroxy atorvastatin, *ortho*-hydroxy atorvastatin acyl glucuronide, and *ortho*-hydroxy atorvastatin ether glucuronide accounting for the majority of radioactivity (Le Couteur et al., 1996). However, the above mentioned glucuronides (G1, G2 and G3) have not been detected in any in vivo samples

and the high instability of G2 under physiologic pH suggest that once formed, it likely contributes mainly to atorvastatin lactonization. In addition, in vitro intrinsic clearance values for atorvastatin and atorvastatin lactone glucuronidation were comparable (Table 1) but significantly lower that those obtained for oxidative metabolism (~ 30-50 μl/min/mg acid; 900-3000 μl/min/mg lactone) (Jacobsen et al., 2000). However, since relative UGT expression levels in human liver are unknown, it complicates the scaling of phase I and phase II metabolism to overall clearance. Collectively, these findings suggest that glucuronidation may contribute to a significant portion of hepatic atorvastatin lactonization and overall atorvastatin clearance.

Based on experiments with recombinant enzymes both atorvastatin and atorvastatin lactone are glucuronidated (G2 and G3) by multiple UGTs including UGT 1A1, 1A3, 1A4, 1A8, and 2B7. The highest rates of lactonization or atorvastatin lactone glucuronidation activity were mediated by UGT1A1 and UGT1A3, or UGT1A3 and UGT1A4, respectively (Fig. 7). The formation of the minor atorvastatin glucuronide (G1) was mediated by UGTs 1A3, 1A4, and 1A9. It has previously been shown that atorvastatin lactonization is mediated by UGT1A1 and UGT1A3, although only six of the twelve currently available UGTs were evaluated (Prueksaritanont et al., 2002a). UGT reaction phenotyping, compared to cytochrome P450, has received less attention due to a lower risk of UGT-mediated drug-drug interactions (Williams et al., 2004). Accordingly, selective probe substrates and/or chemical inhibitors useful in determining relative importance of UGTs responsible for atorvastatin glucuronidation are not currently available (Miners et al., 2004). Evidence for high turnover by individual recombinant UGTs (Fig. 7) does not necessarily imply relative contributions in human liver or extrahepatic tissues since enzyme preparations are standardized to protein content and the tools available to determine relative hepatic or extrahepatic levels of individual UGTs in subcellular human tissue

fractions are lacking. Currently, out of the 18 known human nucleotide sequences encoding UGT enzymes, hepatic isoforms that are not available include UGT2B10, UGT2B11 and UGT2B28 (Miners et al., 2004). Nevertheless, our data suggests that at least six UGT enzymes could contribute towards atorvastatin glucuronidation, which reduces potential drug-drug interaction risk through inhibition of a single enzymatic pathway (Williams et al., 2004).

Atorvastatin lactonization was inhibited by gemfibrozil as well as fenofibrate and its active metabolite, fenofibric acid, with similar apparent inhibitory potencies (Table 1). This is in contrast to previous studies that reported no inhibition by fenofibrate (75 μM), which was proposed as explanation for a differential fibrate interaction with statins in the clinic (Prueksaritanont et al., 2002b). In the presence of increasing concentrations of gemfibrozil, fenofibrate, or fenofibric acid, the formation of G1 increased 1.6-fold, 6.7-fold and 9.5-fold, respectively (Fig. 8). The increase in G1 formation may be attributed to metabolic shunting and/or heterotropic enzyme activation commonly observed with UGTs (Williams et al., 2002; Miners et al., 2004). The significantly larger increase in G1 formation in the presence of fenofibrate and fenofibric acid may reflect their ability to inhibit a parallel glucuronidation pathway (G3) while atorvastatin lactone glucuronidation was relatively insensitive to inhibition by gemfibrozil (Fig. 8).

In order to predict the extent of a pharmacokinetic interaction between atorvastatin and gemfibrozil or fenofibrate, a similar approach previously used for cytochrome P450 enzymes was applied (Brown et al., 2005). Assuming that inhibition of glucuronidation plays role in the mechanism of the pharmacokinetic interaction, clinical differences in the ability of these fibrates to influence atorvastatin pharmacokinetics likely relates to relative differences in hepatic fibrate exposure, since a differential ability to inhibit in vitro glucuronidation was not observed in this

study. Following oral administration, total drug (bound and unbound) peak plasma concentrations (C_{max}) of gemfibrozil and fenofibric acid are in the order of 80 μM and 30 μM following administration 600 mg BID or 160 mg QD, respectively (Miller and Spence, 1998; Schneck et al., 2004). Initial predictions using total drug concentrations as currently recommended by draft FDA guidance, predicted a small gemfibrozil and fenofibric acid interaction. However, both gemfibrozil and fenofibric acid are extensively bound to plasma proteins (>98%) resulting in maximum unbound plasma concentrations of approximately 1.6 μM and 0.3 μM, respectively (Miller and Spence, 1998). Circulating drug levels are therefore much lower than the IC_{50}s for atorvastatin lactonization obtained in this study (Table 1), consistent with previously reported IC_{50} values obtained for gemfibrozil in HLM (316 μM) or hepatocytes (63 μM) (Prueksaritanont et al., 2002b). More sophisticated predictions for drug-drug interactions were obtained by incorporating unbound inhibitor concentration at the inlet to the liver and inhibitor absorption rate constant (Brown et al., 2005). When these values are used to predict the likelihood of a drug-drug interaction between atorvastin and fibrates, a small increase in atorvastatin AUC is predicted with gemfibrozil (~ 1.2-fold) and no interaction following fenofibrate co-administration (Table 3). In comparison, a small gemfibrozil interaction (~ 1.3-fold) and lesser fenofibrate interaction (~1.1-fold) are predicted using total drug peak plasma concentrations. The former method employing unbound plasma fibrate concentration at the inlet to the liver is also believed to be of physiological relevance (Kanamitsu et al., 2000). Recently, small changes in atorvastatin AUC (1.35-fold) were reported following co-administration of atorvastatin (40 mg) with gemfibrozil (600 mg twice daily) and no significant change when administered with fenofibrate (160 mg daily) (Whitfield et al., 2005). The modest interaction between atorvastatin and gemfibrozil was also observed in another study indicating a minimal

change in atorvastatin AUC (1.24-fold) at a lower atorvastatin dose (20 mg) following co-administration with gemfibrozil (Backman et al., 2005). The atorvastatin lactone/atorvastatin AUC ratio also decreased (~20% to 35%) during gemfibrozil co-administration while AUC ratios for hydroxylated metabolites/atorvastatin increased (~25% to 50%), suggesting inhibition of glucuronidation (lactonization) and shunting towards oxidative metabolism (Backman et al., 2005; Whitfield et al., 2005). Therefore, based on the these predictions, inhibition of statin glucuronidation is likely to contribute to a lesser drug-drug interaction between atorvastatin and gemfibrozil, compared to the observed pharmacokinetic interaction between gemfibrozil and other statins.

In summary, gemfibrozil and fenofibrate are weak and non-selective inhibitors of atorvastatin lactonization. Based on the in vitro findings, the likelihood for a significant pharmacokinetic interaction between atorvastatin and these fibrates due to inhibition of glucuronidation is low (Williams et al., 2004). This is based on the observation that multiple UGT enzymes contribute towards atorvastatin glucuronidation, the possibility of metabolic shunting, weak in vitro inhibition potency and lack of differentiation in the ability of gemfibrozil or fenofibric acid to inhibit atorvastatin glucuronidation, and comparable clinical plasma exposure to gemfibrozil and fenofibric acid. However, based on unbound fibrate concentrations at the inlet to the liver, the observed inhibition of atorvastatin glucuronidation by fibrates in HLM predicts a small increase in atorvastatin AUC (~ 1.2-fold) when co-administered with gemfibrozil and no interaction with fenofibrate. These findings are consistent with clinical finding indicating minimal increases in atorvastatin AUC (~ 1.2- to 1.4 fold) observed during co-administration with gemfibrozil and no change with fenofibrate (Backman et al., 2005; Whitfield et al., 2005).

References

Backman JT, Kyrklund C, Kivisto KT, Wang JS and Neuvonen PJ (2000) Plasma concentrations of active simvastatin acid are increased by gemfibrozil. *Clin Pharmacol Ther* **68:**122-129.

Backman JT, Kyrklund C, Neuvonen M and Neuvonen PJ (2002) Gemfibrozil greatly increases plasma concentrations of cerivastatin. *Clin Pharmacol Ther* **72:**685-691.

Backman JT, Luurila H, Neuvonen M and Neuvonen PJ (2005) Rifampin markedly decreases and gemfibrozil increases the plasma concentrations of atorvastatin and its metabolites. *Clin Pharmacol Ther* **78:**154-167.

Bays H (2006) Statin safety: an overview and assessment of the data--2005. *Am J Cardiol* **97:**6C-26C.

Bergman AJ, Murphy G, Burke J, Zhao JJ, Valesky R, Liu L, Lasseter KC, He W, Prueksaritanont T, Qiu Y, Hartford A, Vega JM and Paolini JF (2004) Simvastatin does not have a clinically significant pharmacokinetic interaction with fenofibrate in humans. *J Clin Pharmacol* **44:**1054-1062.

Bottorff MB (2006) Statin safety and drug interactions: clinical implications. *Am J Cardiol* **97:**27C-31C.

Brown HS, Ito K, Galetin A and Houston JB (2005) Prediction of in vivo drug-drug interactions from in vitro data: impact of incorporating parallel pathways of drug elimination and inhibitor absorption rate constant. *Br J Clin Pharmacol* **60:**508-518.

Chen C, Mireles RJ, Campbell SD, Lin J, Mills JB, Xu JJ and Smolarek TA (2005) Differential interaction of 3-hydroxy-3-methylglutaryl-CoA reductase inhibitors with ABCB1, ABCC2, and OATP1B1. *Drug Metab Dispos* **33:**537-546.

Grundy SM, Cleeman JI, Merz CN, Brewer HB, Jr., Clark LT, Hunninghake DB, Pasternak RC, Smith SC, Jr. and Stone NJ (2004) Implications of recent clinical trials for the National Cholesterol Education Program Adult Treatment Panel III guidelines. *Circulation* **110:**227-239.

Guyton JR (2006) Benefit versus risk in statin treatment. *Am J Cardiol* **97:**95C-97C.

Jacobsen W, Kuhn B, Soldner A, Kirchner G, Sewing KF, Kollman PA, Benet LZ and Christians U (2000) Lactonization is the critical first step in the disposition of the 3-hydroxy-3-methylglutaryl-CoA reductase inhibitor atorvastatin. *Drug Metab Dispos* **28:**1369-1378.

Kanamitsu S, Ito K and Sugiyama Y (2000) Quantitative prediction of in vivo drug-drug interactions from in vitro data based on physiological pharmacokinetics: use of maximum unbound concentration of inhibitor at the inlet to the liver. *Pharm Res* **17:**336-343.

Kantola T, Kivisto KT and Neuvonen PJ (1998) Effect of itraconazole on the pharmacokinetics of atorvastatin. *Clin Pharmacol Ther* **64:**58-65.

Kearney AS, Crawford LF, Mehta SC and Radebaugh GW (1993) The interconversion kinetics, equilibrium, and solubilities of the lactone and hydroxyacid forms of the HMG-CoA reductase inhibitor, CI-981. *Pharm Res* **10:**1461-1465.

Kyrklund C, Backman JT, Kivisto KT, Neuvonen M, Laitila J and Neuvonen PJ (2001) Plasma concentrations of active lovastatin acid are markedly increased by gemfibrozil but not by bezafibrate. *Clin Pharmacol Ther* **69:**340-345.

Kyrklund C, Backman JT, Neuvonen M and Neuvonen PJ (2003) Gemfibrozil increases plasma pravastatin concentrations and reduces pravastatin renal clearance. *Clin Pharmacol Ther* **73:**538-544.

Lau YY, Huang Y, Frassetto L and Benet LZ (2007) Effect of OATP1B transporter inhibition on the pharmacokinetics of atorvastatin in healthy volunteers. *Clin Pharmacol Ther* **81:**194-204.

Law M and Rudnicka AR (2006) Statin safety: a systematic review. *Am J Cardiol* **97:**52C-60C.

Le Couteur DG, Martin PF, Pond SM, Bracs P, Black A, Hayes R, Woolf TF and Stern R (1996) Metabolism and excretion of ^{14}C atorvastatin in patients with T-tube drainage (Abstract). *Proc Aust Soc Clin Exp Pharmacol Toxicol* **3:**153.

Lennernas H (2003) Clinical pharmacokinetics of atorvastatin. *Clin Pharmacokinet* **42:**1141-1160.

Li C, Subramanian R, Yu S and Prueksaritanont T (2006) Acyl-coenzyme A formation of simvastatin in mouse liver preparations. *Drug Metab Dispos* **34:**102-110.

Martin PD, Dane AL, Schneck DW and Warwick MJ (2003) An open-label, randomized, three-way crossover trial of the effects of coadministration of rosuvastatin and fenofibrate on the pharmacokinetic properties of rosuvastatin and fenofibric acid in healthy male volunteers. *Clin Ther* **25:**459-471.

Mathew P, Cuddy T, Tracewell WG and Salazar D (2004) An open-label study on the pharmacokinetics (PK) of pitavastatin (NK-104) when administered concomitantly with fenofibrate or gemfibrozil in healthy volunteers (Abstract PI-115). *Clin Pharmacol Ther* **75:**P33.

Miller DB and Spence JD (1998) Clinical pharmacokinetics of fibric acid derivatives (fibrates). *Clin Pharmacokinet* **34:**155-162.

Miners JO, Smith PA, Sorich MJ, McKinnon RA and Mackenzie PI (2004) Predicting human drug glucuronidation parameters: application of in vitro and in silico modeling approaches. *Annu Rev Pharmacol Toxicol* **44:**1-25.

Newman CB, Palmer G, Silbershatz H and Szarek M (2003) Safety of atorvastatin derived from analysis of 44 completed trials in 9,416 patients. *Am J Cardiol* **92:**670-676.

Pan WJ, Gustavson LE, Achari R, Rieser MJ, Ye X, Gutterman C and Wallin BA (2000) Lack of a clinically significant pharmacokinetic interaction between fenofibrate and pravastatin in healthy volunteers. *J Clin Pharmacol* **40:**316-323.

Prueksaritanont T, Subramanian R, Fang X, Ma B, Qiu Y, Lin JH, Pearson PG and Baillie TA (2002a) Glucuronidation of statins in animals and humans: a novel mechanism of statin lactonization. *Drug Metab Dispos* **30:**505-512.

Prueksaritanont T, Tang C, Qiu Y, Mu L, Subramanian R and Lin JH (2002b) Effects of fibrates on metabolism of statins in human hepatocytes. *Drug Metab Dispos* **30:**1280-1287.

Prueksaritanont T, Zhao JJ, Ma B, Roadcap BA, Tang C, Qiu Y, Liu L, Lin JH, Pearson PG and Baillie TA (2002c) Mechanistic studies on metabolic interactions between gemfibrozil and statins. *J Pharmacol Exp Ther* **301:**1042-1051.

Rowland M and Matin SB (1973) Kinetics of drug-drug interactions. *J Pharmacokinet Biopharm* **1:**553-567.

Rubins HB, Robins SJ, Collins D, Fye CL, Anderson JW, Elam MB, Faas FH, Linares E, Schaefer EJ, Schectman G, Wilt TJ and Wittes J (1999) Gemfibrozil for the secondary prevention of coronary heart disease in men with low levels of high-density lipoprotein cholesterol. Veterans Affairs High-Density Lipoprotein Cholesterol Intervention Trial Study Group. *N Engl J Med* **341:**410-418.

Schneck DW, Birmingham BK, Zalikowski JA, Mitchell PD, Wang Y, Martin PD, Lasseter KC, Brown CD, Windass AS and Raza A (2004) The effect of gemfibrozil on the pharmacokinetics of rosuvastatin. *Clin Pharmacol Ther* **75:**455-463.

Shitara Y and Sugiyama Y (2006) Pharmacokinetic and pharmacodynamic alterations of 3-hydroxy-3-methylglutaryl coenzyme A (HMG-CoA) reductase inhibitors: drug-drug interactions and interindividual differences in transporter and metabolic enzyme functions. *Pharmacol Ther* **112:**71-105.

Spence JD, Munoz CE, Hendricks L, Latchinian L and Khouri HE (1995) Pharmacokinetics of the combination of fluvastatin and gemfibrozil. *Am J Cardiol* **76:**80A-83A.

Vasudevan AR and Jones PH (2006) Effective use of combination lipid therapy. *Curr Atheroscler Rep* **8:**76-84.

Whitfield LR, Abel R, Hartman D, Porcari A and Alvey C (2005) Effects of co-administration of gemfibrozil and fenofibrate on the pharmacokinetic profile of atorvastatin and major metabolites (Abstract 547-P). *Diabetes* **54:**A135.

Williams JA, Hyland R, Jones BC, Smith DA, Hurst S, Goosen TC, Peterkin V, Koup JR and Ball SE (2004) Drug-drug interactions for UDP-glucuronosyltransferase substrates: a pharmacokinetic explanation for typically observed low exposure (AUCi/AUC) ratios. *Drug Metab Dispos* **32:**1201-1208.

Williams JA, Ring BJ, Cantrell VE, Campanale K, Jones DR, Hall SD and Wrighton SA (2002) Differential modulation of UDP-glucuronosyltransferase 1A1 (UGT1A1)-catalyzed estradiol-3-glucuronidation by the addition of UGT1A1 substrates and other compounds to human liver microsomes. *Drug Metab Dispos* **30:**1266-1273.

Wu X, Whitfield LR and Stewart BH (2000) Atorvastatin transport in the Caco-2 cell model: contributions of P-glycoprotein and the proton-monocarboxylic acid co-transporter. *Pharm Res* **17:**209-215.

Footnotes

This work was presented in part at the 2007 Annual Meeting of the American Society for Clinical Pharmacology and Therapeutics, March 21-24, 2007, Anaheim, CA.

[1] Current affiliation: Amgen Inc., Seattle, WA.

[2] Current affiliation: Schering-Plough, Kenilworth, NJ.

Legends for figures

Fig. 1. Proposed glucuronidation pathways of atorvastatin following incubation with human liver microsomes.

Fig. 2. Representative HPLC-UV (A) and β-RAM (B) profiles of a HLM incubate with [^{3}H]atorvastatin (10 μM) and UDPGA (5 mM), and representative HPLC-UV profile following HLM incubation with atorvastatin lactone (10 μM) and UDPGA (5 mM) (C).

Fig. 3. MS/MS spectra (ESI positive ion mode) of atorvastatin (A), atorvastatin lactone (B), atorvastatin glucuronide (C) and atorvastatin lactone glucuronide (D).

Fig. 4. Enzyme kinetics of atorvastatin lactonization by pooled HLMs in Tris-HCl buffer (pH 7.0) displaying substrate inhibition at higher atorvastatin concentrations. Eadie-Hofstee plot is shown as insert to illustrate inhibition kinetics.

Fig. 5. Enzyme kinetics of atorvastatin acyl glucuronide (G2) formation by pooled HLMs in Tris-HCl buffer (pH 7.0) displaying substrate inhibition at higher atorvastatin concentrations. Eadie-Hofstee plot is shown as insert to illustrate inhibition kinetics.

Fig. 6. Enzyme kinetics of atorvastatin lactone glucuronidation (G3) by pooled HLMs in Tris-HCl buffer (pH 7.0) displaying typical Michalis-Menten kinetics. Eadie-Hofstee plot is shown as insert.

Fig. 7. Formation of atorvastatin glucuronides (G1 and G2) from atorvastatin (1, 10 μM) and atorvastatin lactone glucuronide (G3) from atorvastatin lactone (1, 10 μM) in the presence of various rUGTs (*Asterisk* indicates low but detectable activity).

Fig. 8. Modulation of atorvastatin glucuronidation (G1 formation and lactonization) and atorvastatin lactone glucuronidation (G3 formation) by gemfibrozil (A, B, C) and fenofibrate (D, E, F), respectively.

Fenofibric acid modulation of atorvastatin glucuronidation was almost identical to fenofibrate.

DMD Fast Forward. Published on April 30, 2007 as DOI: 10.1124/dmd.107.015230
This article has not been copyedited and formatted. The final version may differ from this version.

Tables

TABLE 1: Kinetic parameters for the glucuronidation of atorvastatin and atorvastatin lactone following incubation with human liver microsomes.

HLM (0.25 mg/mL) were pretreated with alamethicin (50 μg/mg protein) and incubated with increasing concentrations of either atorvastatin or atorvastatin lactone (0.1-300 μM) in Tris-HCl buffer to determine kinetic parameters. Values represent mean parameter estimates ± SEM from three experiments.

Product[a]	K_m	V_{max}	K_i[b]	CL_{int}
	μM	*pmol/min/mg*	*μM*	*μl/min/mg*
Lactonization	12 ± 3.7	74 ± 13	75 ± 29	6.2
G2	28 ± 4.5	NA	36 ± 5.8	NA
G3	2.6 ± 0.3	11 ± 0.3	NA	4.2

[a] Lactonization is the major glucuronidation pathway for atorvastatin, mediated via acyl glucuronide (G2) formation, calculated from summation of G2 and atorvastatin lactone as products. G3 is the atorvastatin lactone glucuronide.

[b] Lactonization and G2 formation exhibited substrate inhibition kinetics.

DMD Fast Forward. Published on April 30, 2007 as DOI: 10.1124/dmd.107.015230
This article has not been copyedited and formatted. The final version may differ from this version.

TABLE 2: Inhibition of atorvastatin and atorvastatin lactone glucuronidation by gemfibrozil, fenofibrate, and fenofibric acid.

HLM (0.5 mg/mL) were pretreated with alamethicin (50 μg/mg protein) and incubated with increasing concentrations of fibrates (0.03-1000 μM) in Tris-HCl buffer to determine IC_{50}s. Values represent means ± SEM from three experiments.

Pathway[a]	IC_{50}		
	Gemfibrozil	Fenofibrate	Fenofibric Acid
	μM	*μM*	*μM*
G1 formation[b]	Increased 1.6-fold	Increased 6.7-fold	Increased 9.5-fold
Lactonization	346 ± 7	320 ± 6	291 ± 15
G3 formation	NA	~ 1000[c]	~ 1000[c]

[a] G1 is a minor atorvastatin ether glucuronide. Lactonization is the major glucuronidation pathway for atorvastatin, mediated via acyl glucuronide (G2) formation, calculated from summation of G2 and atorvastatin lactone as products. G3 is the atorvastatin lactone glucuronide.

[b] G1 formation was not inhibited by fibrates but generally increased with increasing fibrate concentratrion.

[c] Mean inhibition as 45% and 49.9% in the presence of 1000 μM fenofibrate and fenofibric acid, respectively.

DMD Fast Forward. Published on April 30, 2007 as DOI: 10.1124/dmd.107.015230
This article has not been copyedited and formatted. The final version may differ from this version.

TABLE 3: Predicted changes in atorvastatin exposure (AUC) during co-administration with fibrates.

Fibrate	Drug Concentration[a]	Predicted AUC Change	Observed AUC Change[b]
	μM	*fold*	*fold*
Gemfibrozil (600 mg twice daily)	-	-	1.24 - 1.35
Plasma C_{max} (total)	82	1.34	-
Plasma C_{max} (unbound)	1.6	1.01	-
Portal vein (unbound)	41	1.18	-
Fenofibrate (160 mg daily)	-	-	1.03
Plasma C_{max} (total)	27	1.13	-
Plasma C_{max} (unbound)	0.27	1.00	-
Portal vein (unbound)	3.7	1.02	-

[a] Fibrate plasma concentration values were obtained from literature values (Whitfield et al., 2005). Unbound fraction (f_u) for gemfibrozil and fenofibrate were 0.02 and 0.01, respectively.

[b] Clinically observed changes in atorvastatin AUC following co-administration of fibrates were previously reported (Backman et al., 2005; Whitfield et al., 2005).

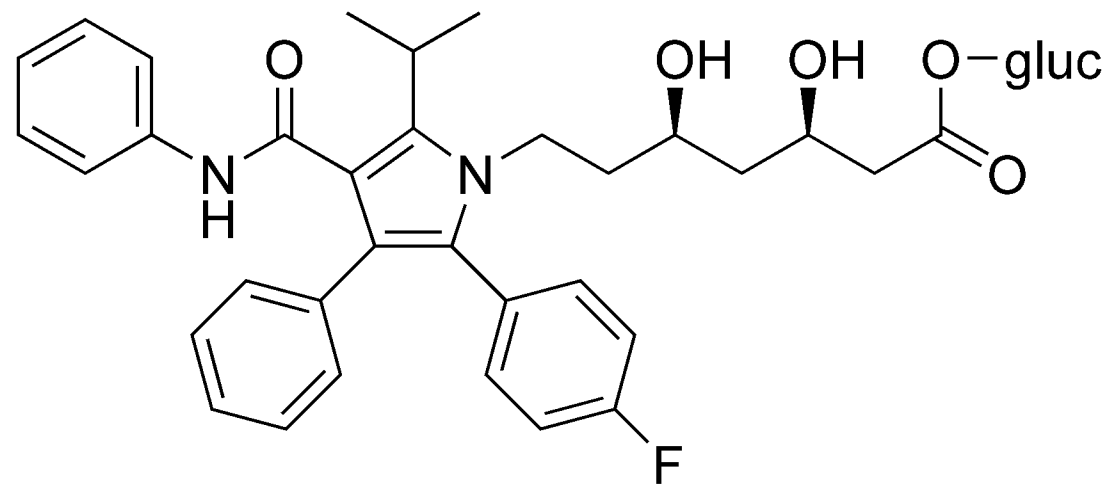

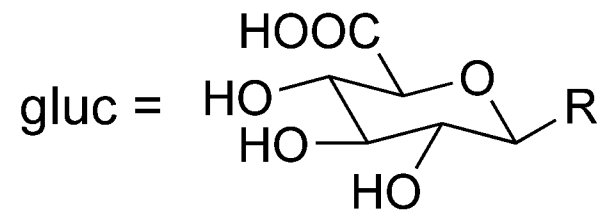

* Position of ^{3}H label

Atorvastatin acyl glucuronide (G2)

UGTs 1A1, A3,
1A4, 1A8, 2B7

Spontaneous

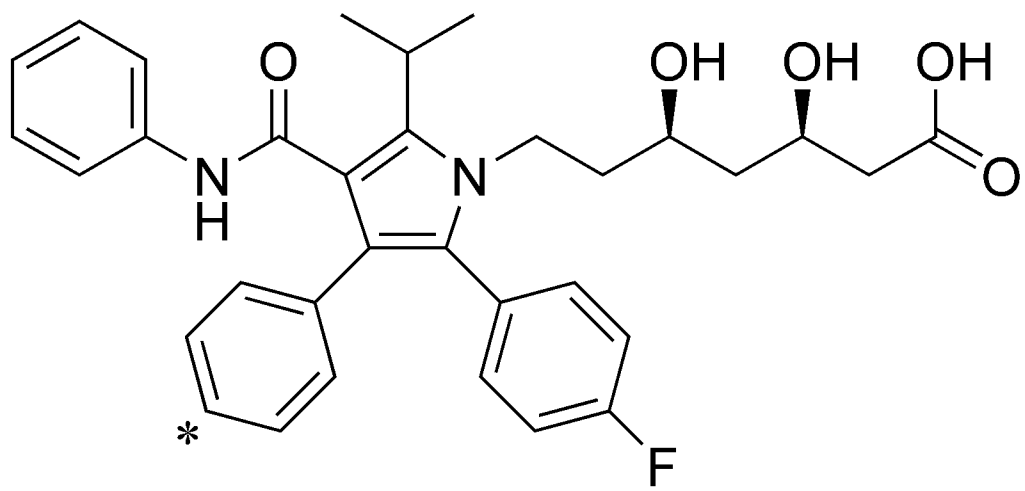

Hydrolysis

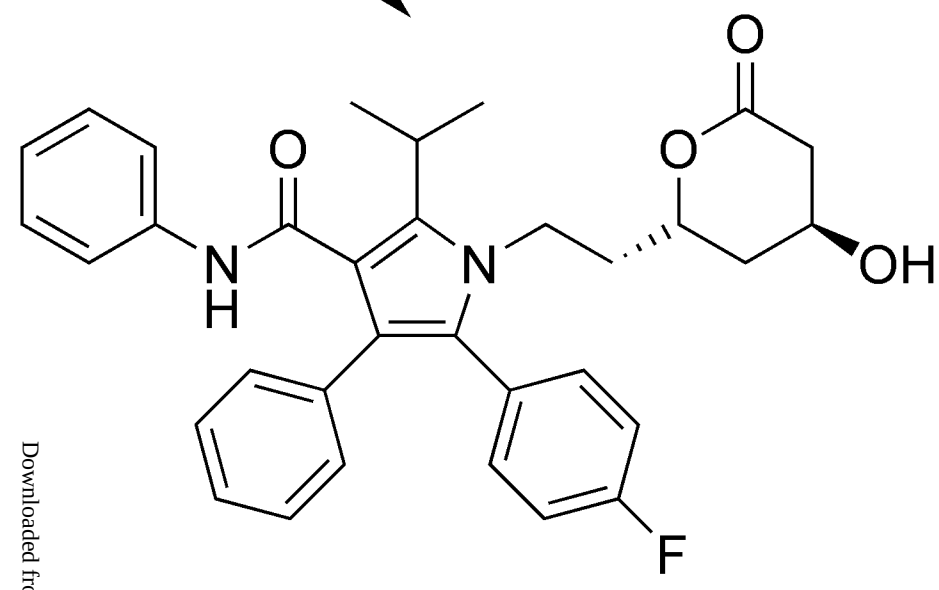

Atorvastatin

UGTs 1A3,
1A4, 1A9

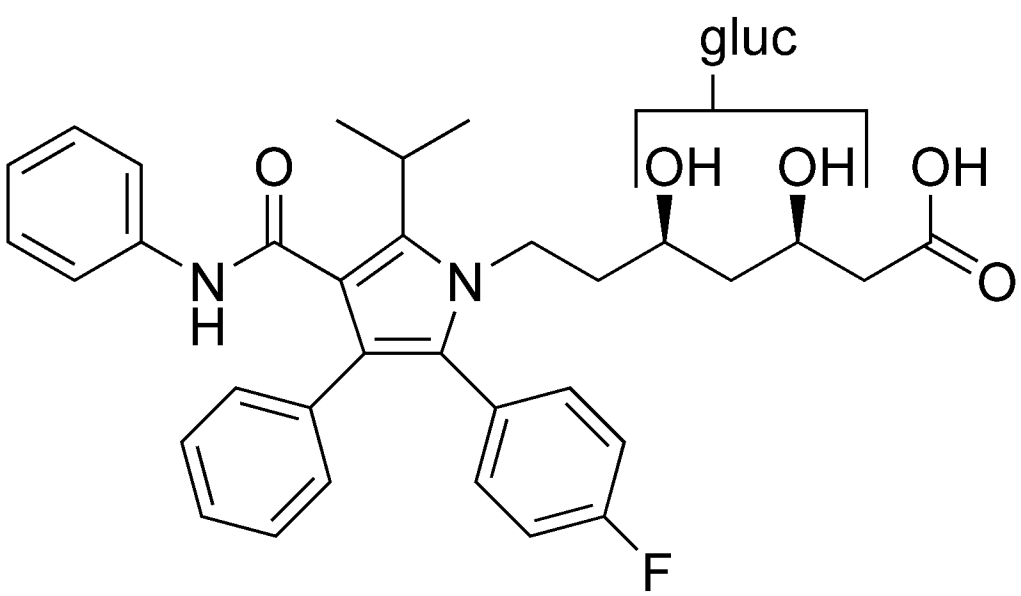

Atorvastatin ether glucuronide (G1)

Atorvastatin lactone

UGTs 1A1, 1A3,
1A4, 1A8, 2B7

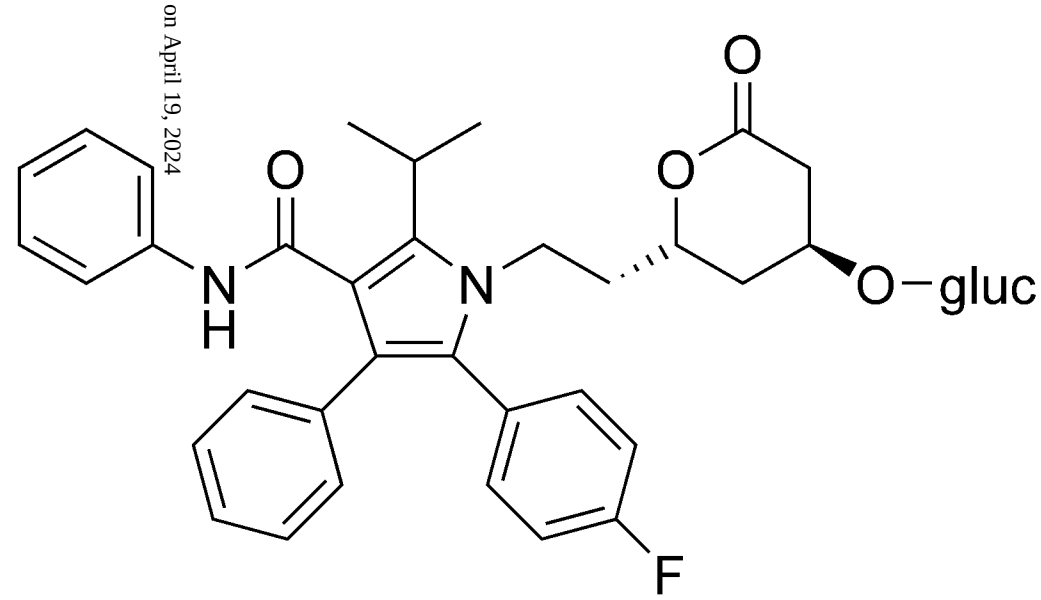

Atorvastatin lactone ether glucuronide (G3)

Figure 1

DMD Fast Forward. Published on April 30, 2007 as DOI: 10.1124/dmd.107.015230
This article has not been copyedited and formatted. The final version may differ from this version.

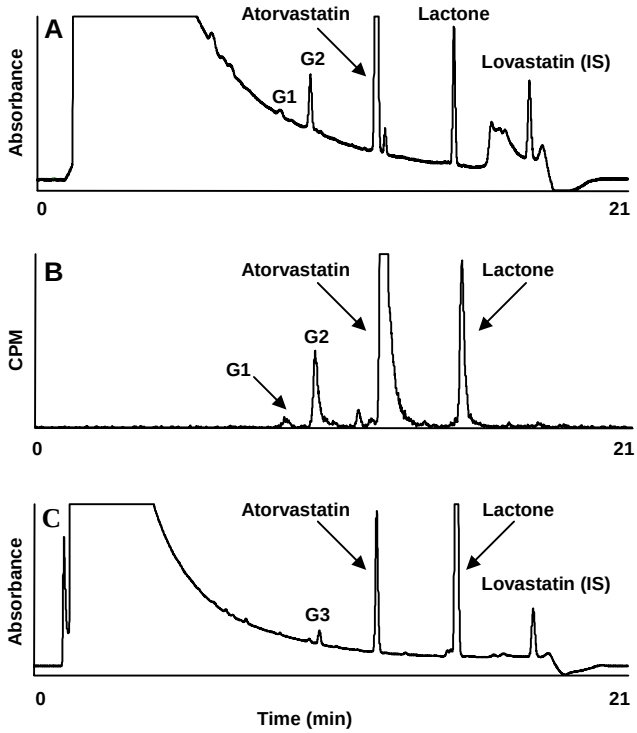

Figure 2

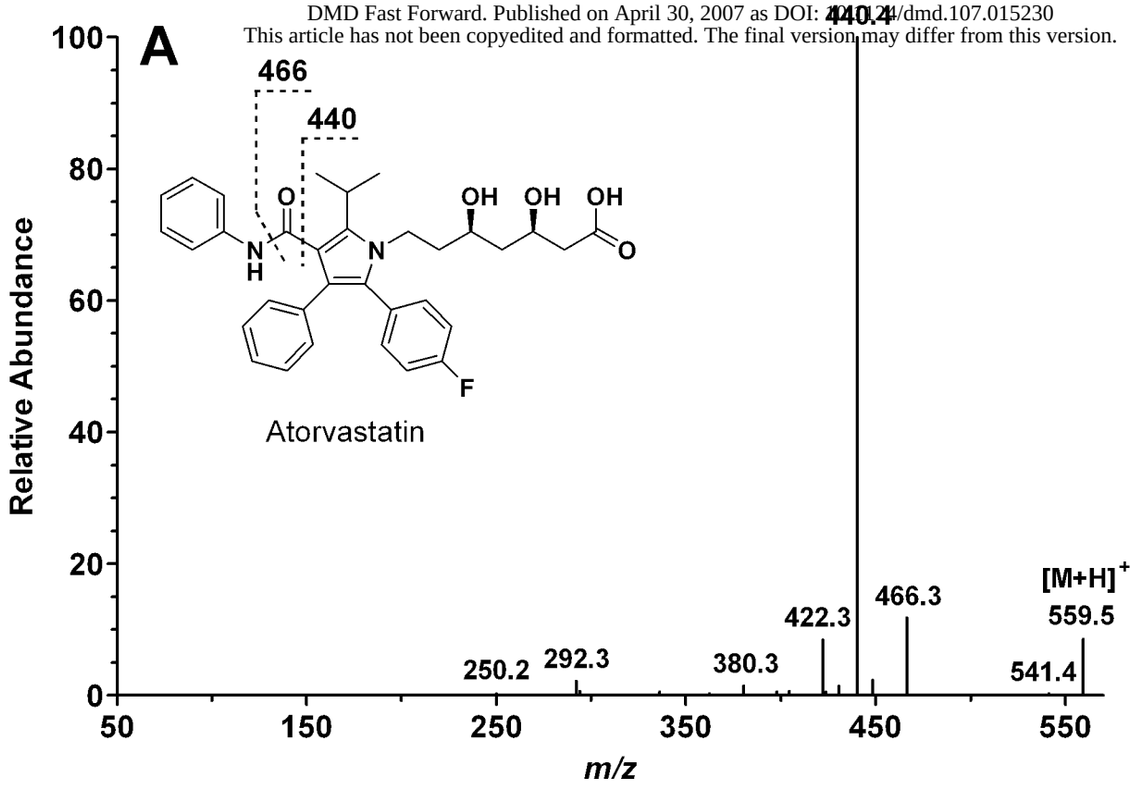

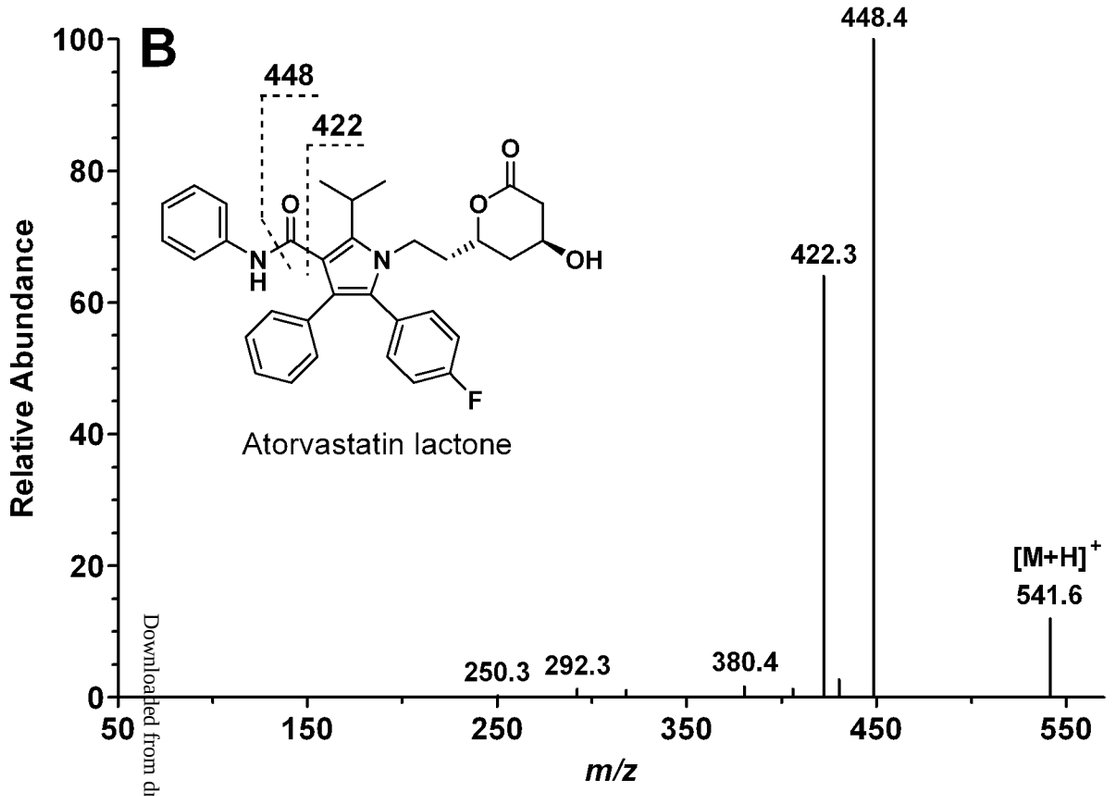

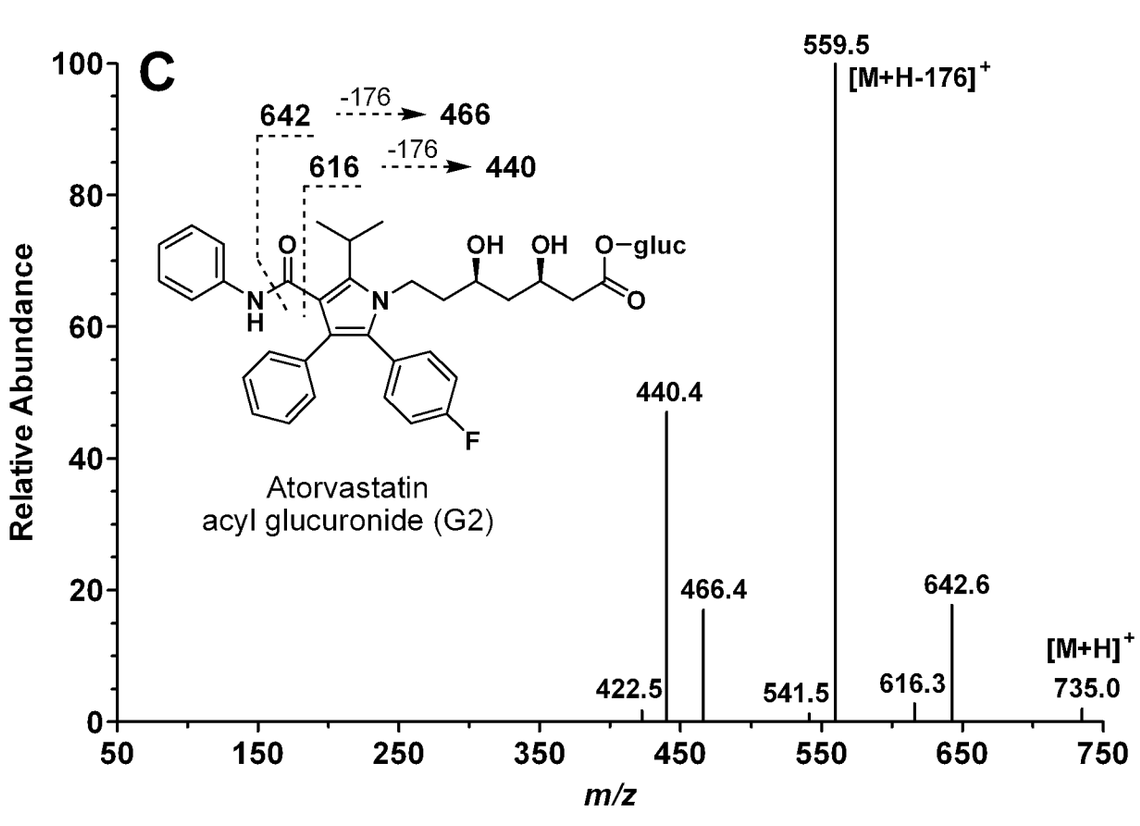

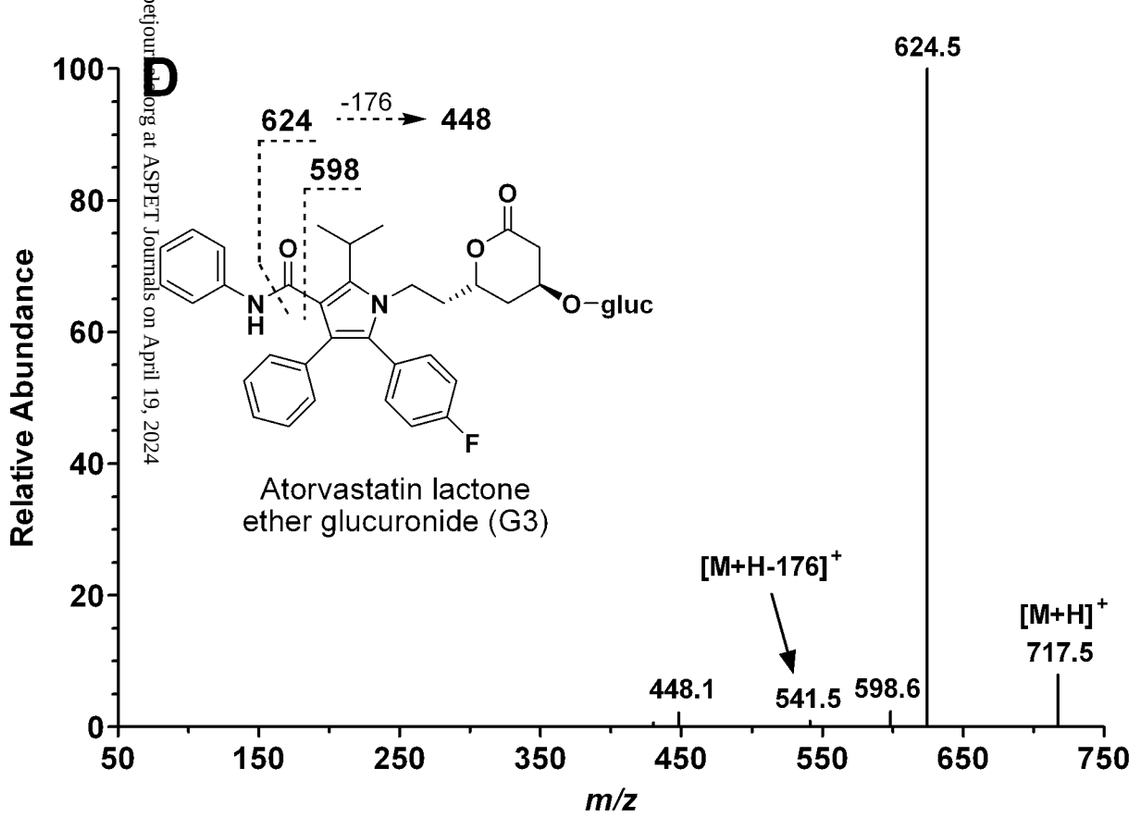

Figure 3

DMD Fast Forward. Published on April 30, 2007 as DOI: 10.1124/dmd.107.015230

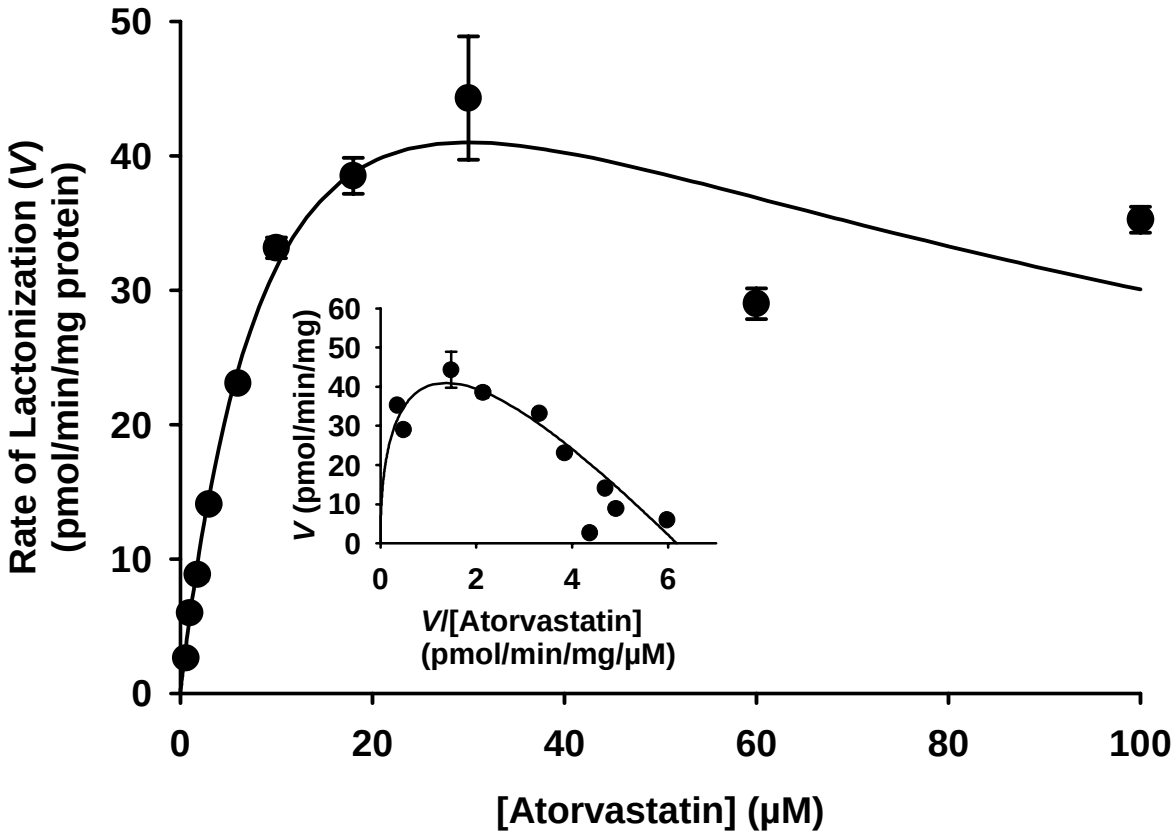

Figure 4

DMD Fast Forward. Published on April 30, 2007 as DOI: 10.1124/dmd.107.015230
This article has not been copyedited and formatted. The final version may differ from this version.

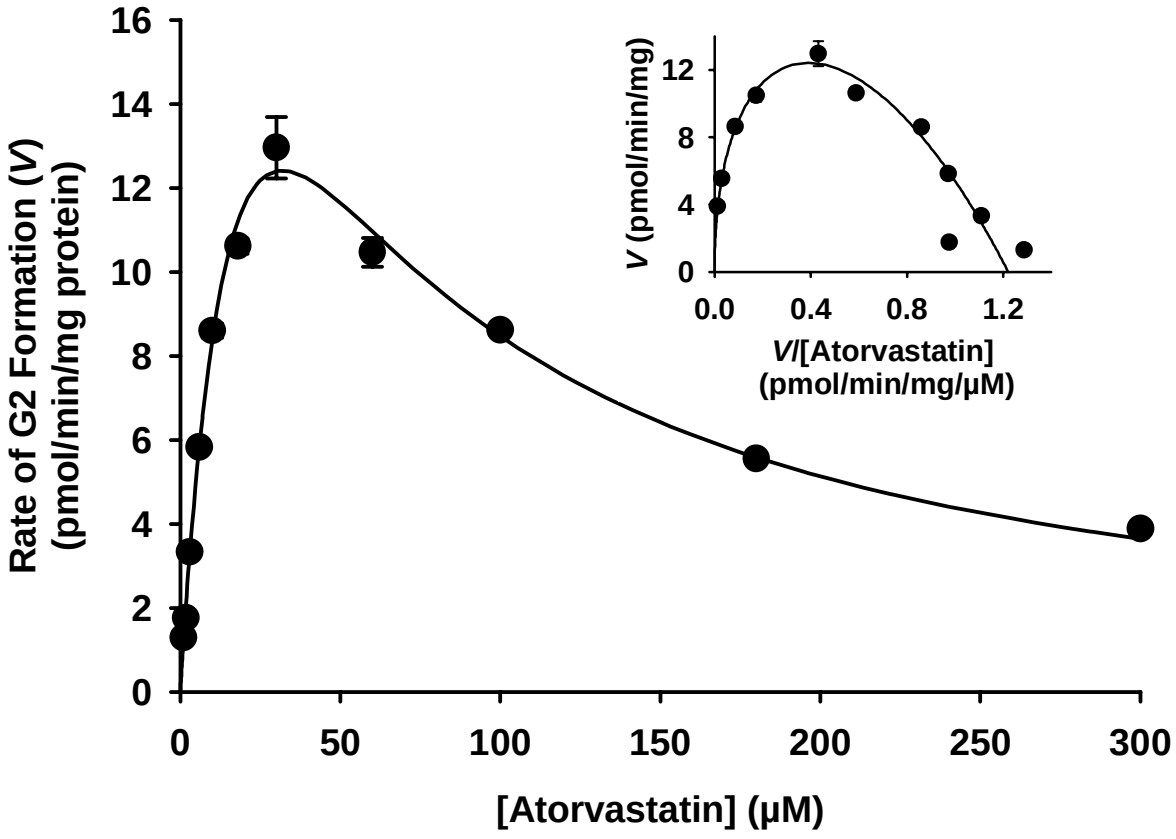

Figure 5

DMD Fast Forward. Published on April 30, 2007 as DOI: 10.1124/dmd.107.015230
This article has not been copyedited and formatted. The final version may differ from this version.

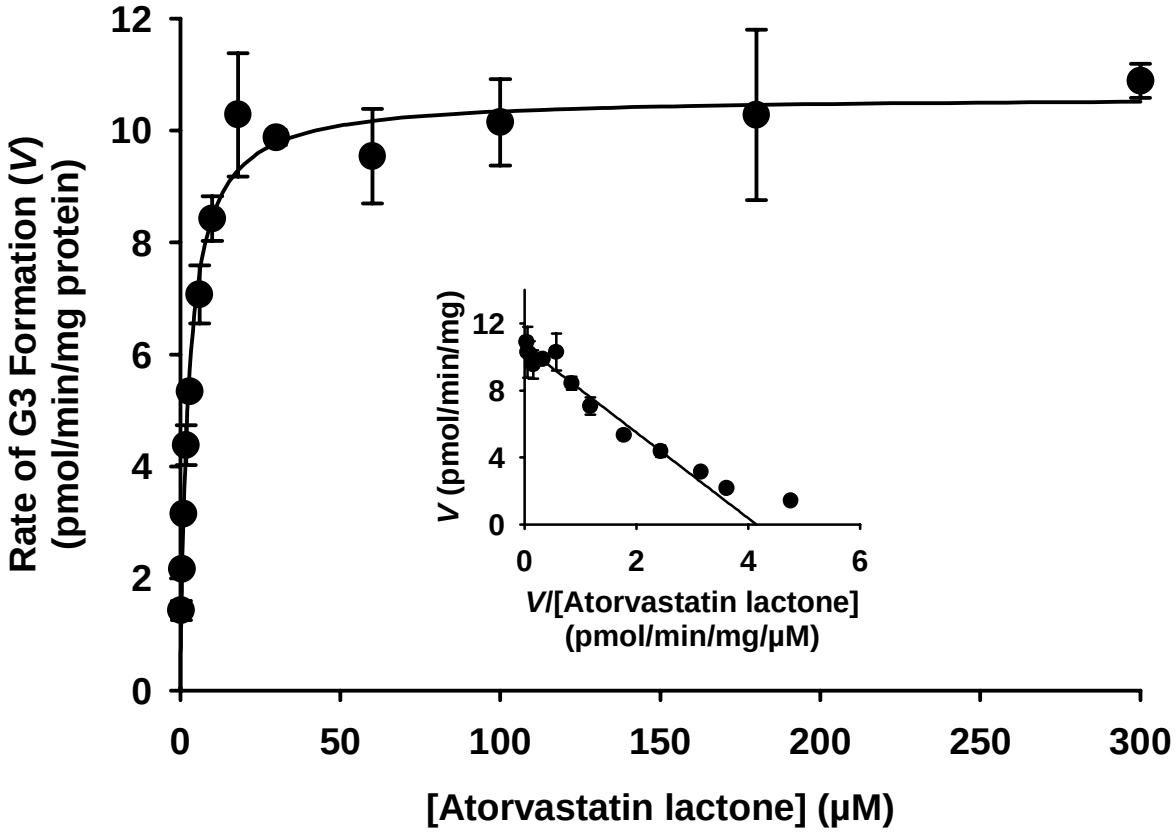

Figure 6

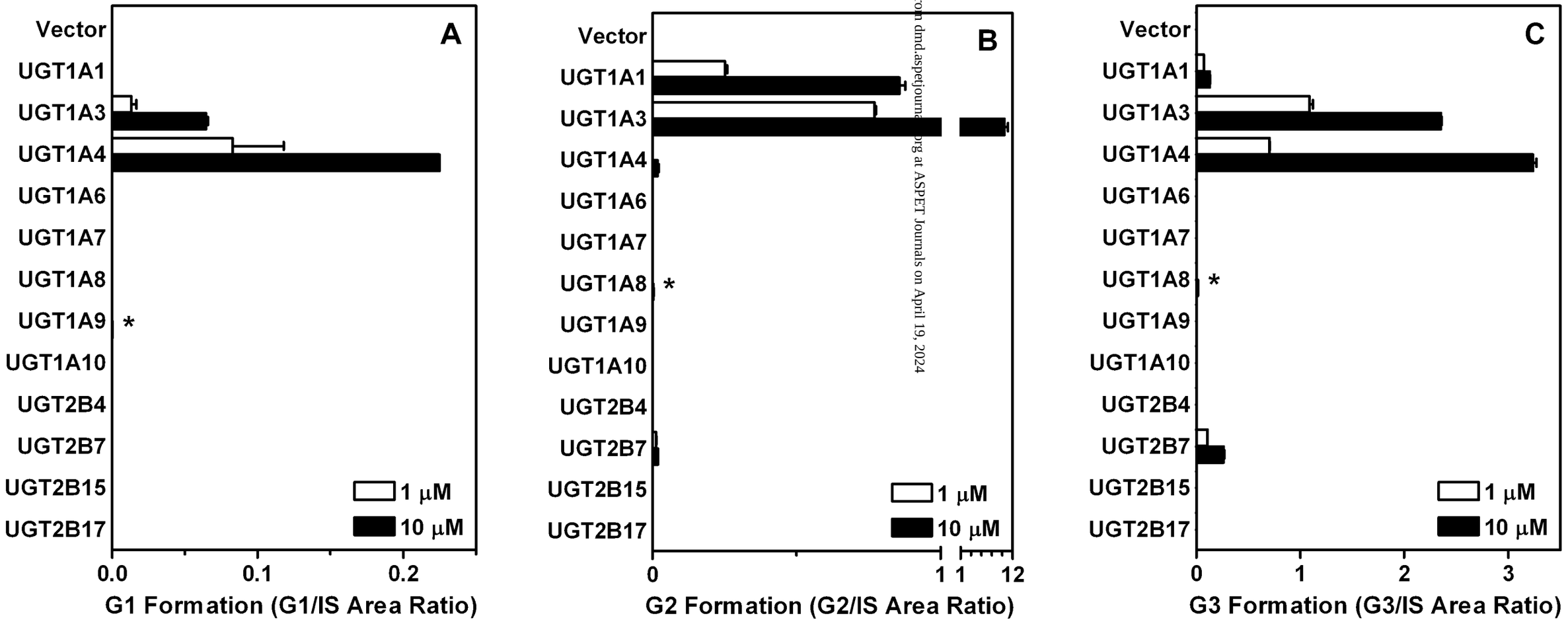

Figure 7

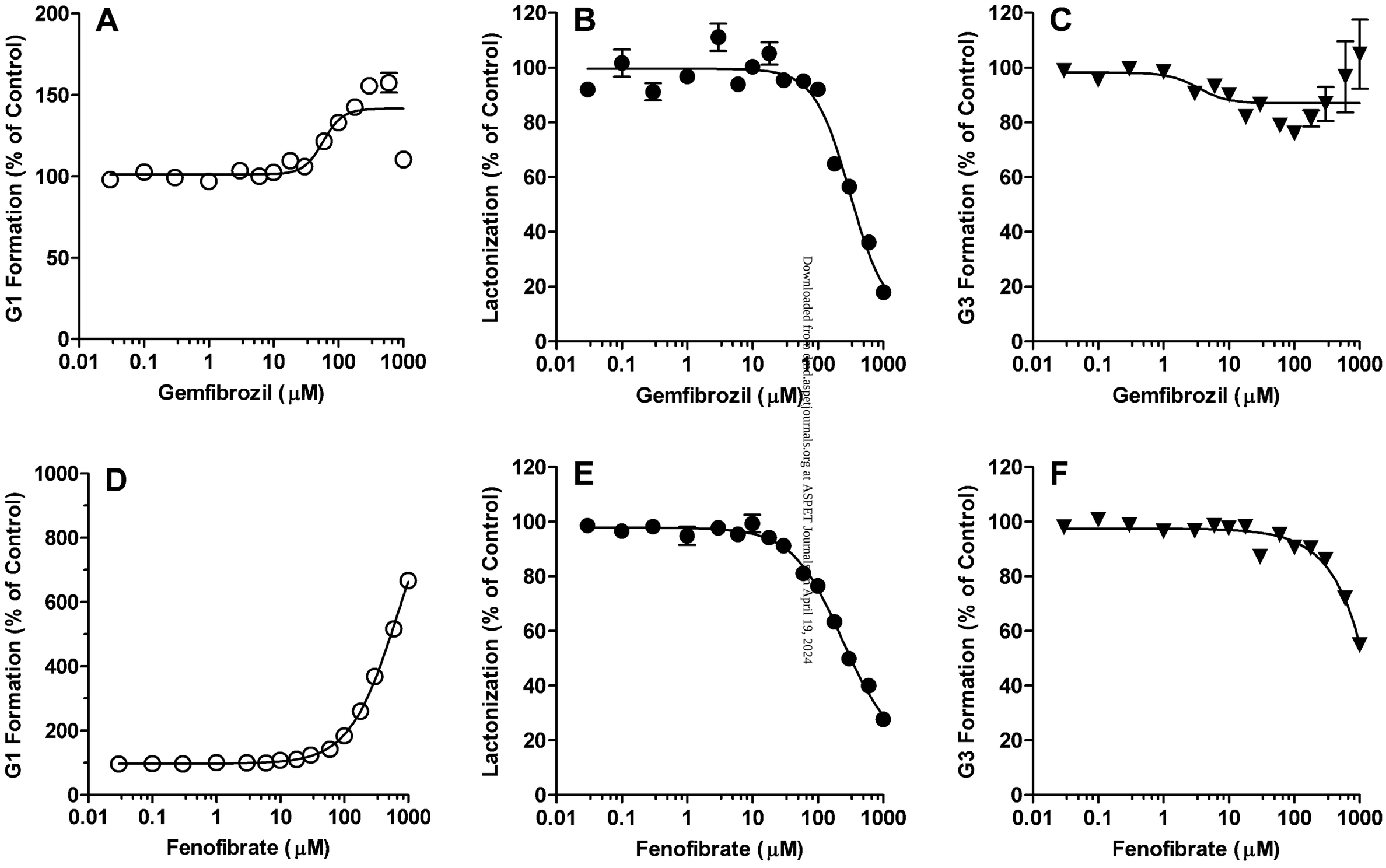

Figure 8